Self-Assembly of Heteronuclear Supramolecular Helical Complexes with Segmental Ligands

Claude Piguet,*,† Gérard Hopfgartner,‡ Bernard Bocquet,† Olivier Schaad,§ and Alan F. Williams†

Contribution from the Department of Inorganic, Analytical and Applied Chemistry and the Department of Biochemistry, University of Geneva, CH-1211 Geneva 4, Switzerland, and Pharma Division, F. Hoffmann-La Roche Ltd, CH-4002 Basel, Switzerland

Received March 29, 1994®

Abstract: The segmental bidentate–tridentate ligand 5-{2′-[6″-(1‴-(3,5-dimethoxybenzyl)-1‴*H*-benzimidazol-2‴-yl)-pyridin-2″-yl]-1′-methyl-1′*H*-benzimidazol-5′-ylmethyl}-1-methyl-2-(6⁗-methylpyridine-2⁗-yl)-1*H*-benzimidazole (L^1) reacts with Fe(II), Zn(II), and Co(II) in acetonitrile to give mononuclear head-to-head complexes $[M(L^1)_2]^{2+}$ where the two tridentate units of the ligands are pseudo-octahedrally coordinated to M(II). Detailed electrospray-mass spectrometeric (ES-MS), spectrophotometric, and ^{1}H-NMR studies show that a second metal ion can react with $[M(L^1)_2]^{2+}$ to give homodinuclear C_2-symmetrical head-to-head double helical complexes $[M_2(L^1)_2]^{4+}$ where the second cation is pseudotetrahedrally bound by the two remaining bidentate units of the ligands. When M = Fe(II), thermodynamic data show that the second metal ion is only weakly coordinated, while for M = Zn(II), Co(II), which display greater affinities for tetrahedral coordination, stable homodinuclear $[M_2(L^1)_2]^{4+}$ are obtained in acetonitrile. Reaction of $[Fe(L^1)_2]^{2+}$ with Ag(I) produces the self-assembled C_2-symmetrical heterodinuclear double-helical complex $[FeAg(L^1)_2]^{3+}$ where Fe(II) occupies the pseudo-octahedral site defined by the two tridentate units of the ligands and Ag(I) lies in the remaining pseudotetrahedral site. Similarly, the trileptic ligand 1,1′-dimethyl-2,2′-bis[6-(methylpyridin-2-yl)-5,5′-{pyridine-2,6-diylbis[(1-methyl-1*H*-benzimidazole-2,5-diyl)methylene]}bis[1*H*-benzimidazole] (L^2) reacts with Fe(II) and Ag(I) (stoichiometric ratio 1:2) to give the first self-assembled D_2-symmetrical heterotrinuclear complex $[FeAg_2(L^2)_2]^{4+}$ where Fe(II) is located in the central pseudo-octahedral site (bistridentate) and Ag(I) occupy the two capping pseudotetrahedral sites. ^{1}H-NMR measurements are compatible with a double-helical or a catenate structure for $[FeAg_2(L^2)_2]^{4+}$. The selectivity of the self-assembly processes is discussed together with thermodynamic and structural factors required for the formation of helical heteropolynuclear complexes.

Introduction

The development of supramolecular devices working on the nanometric scale is the subject of intense research.[1-3] Molecular shuttles,[4,5] photoswitches,[6] light conversion,[7] and electron transfer[8] devices have been obtained through the assembly of the various necessary components into well-defined supramolecular architectures. In many cases[7-9] the planned device requires the preparation of heteropolynuclear complexes which are not statistical mixtures,[7,9,10] and the use of highly selective self-assembly processes recently developed for the synthesis of double[11-14] and triple-helical[15,16] polynuclear complexes offer new possibilities in this domain.

It has been shown[9,11-16] that a good matching of the ligand binding possibilities and the stereochemical preferences of the metal ions leads to the selective formation of helical polynuclear complexes with well-defined coordination sites. Bidentate donor units combined with tetrahedral metal ions[11-13] or tridentate units with octahedral metal ions[12,13] produce double-helical polynuclear complexes while bidentate binding units combined with octahedral metal ions[15,16] or tridentate units with tricapped trigonal prismatic

† Department of Inorganic, Analytical and Applied Chemistry, Geneva.
‡ Hoffmann-La Roche, Pharma Division, Basel.
§ Department of Biochemistry, Geneva.
• Abstract published in *Advance ACS Abstracts,* September 1, 1994.

(1) Lehn, J.-M. *Angew. Chem., Int. Ed. Engl.* **1990**, *29*, 1304–1319.
(2) Balzani, V. *Tetrahedron* **1992**, *48*, 10443–10514.
(3) Anelli, P. L.; Ashton, P. R.; Ballardini, R.; Balzani, V.; Delgado, M.; Gandolfi, M. T.; Goodnow, T. T.; Kaifer, A. E.; Philp, D.; Pietraszkiewicz, M.; Prodi, L.; Reddington, M. V.; Slawin, A. M. Z.; Spencer, N.; Stoddart, J. F.; Vicent, C.; Williams, D. J. *J. Am. Chem. Soc.* **1992**, *114*, 193–218.
(4) Ballardini, R.; Balzani, V.; Gandolfi, M. T.; Prodi, L.; Venturi, M.; Philip, D.; Ricketts, H. G.; Stoddart, J. F. *Angew. Chem., Int. Ed. Engl.* **1993**, *32*, 1301–1303. Anelli, P. L.; Spencer, N.; Stoddart, J. F. *J. Am. Chem. Soc.* **1991**, *113*, 5131–5133.
(5) Benniston, A. C.; Harriman, A. *Angew. Chem., Int. Ed. Engl.* **1993**, *32*, 1459–1461.
(6) Goulle, V.; Harriman, A.; Lehn, J.-M. *J. Chem. Soc., Chem. Commun.* **1993**, 1034–1036. Jenkins, Y.; Barton, J. K. *J. Am. Chem. Soc.* **1992**, *114*, 8736–8738.
(7) Bünzli, J.-C. G.; Froidevaux, P.; Harrowfield, J. Mac B. *Inorg. Chem.* **1993**, *32*, 3306–3311. Guerriero, P.; Vigato, P. A.; Bünzli, J.-C. G.; Moret, E. *J. Chem. Soc., Dalton Trans.* **1990**, 647–655. Denti, G.; Serroni, S.; Campagna, S.; Juris, A.; Ciano, M.; Balzani, V. In *Perspectives in Coordination Chemistry*; Williams, A. F., Floriani, C., Merbach, A. E., Eds.; VHCA: Basel, 1992; pp 153–164. Sabbatini, N.; Guardigli, M.; Lehn, J.-M. *Coord. Chem. Rev.* **1993**, *123*, 201–228. Pikramenou, Z.; Nocera, D. G. *Inorg. Chem.* **1992**, *31*, 532–536.
(8) Collin, J.-P.; Guillerez, S.; Sauvage, J.-P.; Barigelletti, F.; De Cola, L.; Flamigni, L.; Balzani, V. *Inorg. Chem.* **1992**, *31*, 4112–4117. Gust, D.; Moore, T. A.; Moore, A. L.; MacPherson, A. N.; Lopez, A.; De Graziano, J. M.; Gouni, I.; Bittersmann, E.; Seely, G. R.; Gao, F.; Nieman, R. A.; Ma, X. C.; Demanche, L. J.; Hung, S. C.; Luttrull, D. K.; Lee, S. J.; Kerrigan, P. K. *J. Am. Chem. Soc.* **1993**, *115*, 11141–11152.
(9) Piguet, C.; Bünzli, J.-C. G.; Bernardinelli, G.; Hopfgartner, G.; Williams, A. F. *J. Am. Chem. Soc.* **1993**, *115*, 8197–8206. Bernardinelli, G.; Piguet, C.; Williams, A. F. *Angew. Chem., Int. Ed. Engl.* **1992**, *31*, 1622–1624.
(10) Matthews, K. D.; Fairman, R. A.; Johnson, A.; Spence, K. V. N.; Kahwa, I. A.; McPherson, G. L.; Robothan, H. *J. Chem. Soc., Dalton Trans.* **1993**, 1719–1723. Fraser, C.; Ostrander, R.; Rheingold, A. L.; White, C.; Bosnich, B. *Inorg. Chem.* **1994**, *33*, 324–337.
(11) Lehn, J.-M.; Sauvage, J.-P.; Simon, J.; Ziessel, R.; Piccini-Leopardi, C.; Germain, G.; Declerq, J.-P.; Van Meerssche, M. *Nouv. J. Chim.* **1983**, *7*, 413–420. Gisselbrecht, J.-P.; Gross, M.; Lehn, J.-M.; Sauvage, J.-P.; Simon, J.; Ziessel, R.; Piccini-Leopardi, C.; Arrieta, J. M.; Germain, G.; Van Meerssche, M. *Nouv. J. Chim.* **1984**, *8*, 661–667. Lehn, J.-M.; Rigault, A.; Siegel, J.; Harrowfield, J.; Chevrier, B.; Moras, D. *Proc. Natl. Acad. Sci. U.S.A.* **1987**, *84*, 2565–2569. Lehn, J.-M.; Rigault, A. *Angew. Chem., Int. Ed. Engl.* **1988**, *27*, 1095–1097. Koert, U.; Harding, M. M.; Lehn, J.-M. *Nature* **1990**, *346*, 339–342. Garrett, T. M.; Koert, U.; Lehn, J.-M.; Rigault, A.; Meyer, D.; Fischer, D. *J. Chem. Soc., Chem. Commun.* **1990**, 557–558. Zarges, W.; Hall, J.; Lehn, J.-M. *Helv. Chim. Acta* **1991**, *74*, 1843–1852. Youinou, M.-T.; Ziessel, R.; Lehn, J.-M. *Inorg. Chem.* **1991**, *30*, 2144–2148. Yao, Y.; Perkovic, M. W.; Rillema, D. P.; Woods, C. *Inorg. Chem.* **1992**, *31*, 3956–3962. Crane, J. D.; Sauvage, J.-P. *New. J. Chem.* **1992**, *16*, 649–650.
(12) Constable, E. C. *Tetrahedron* **1992**, *48*, 10013–10059 and references therein.

0002-7863/94/1516-9092$04.50/0

Chart 1

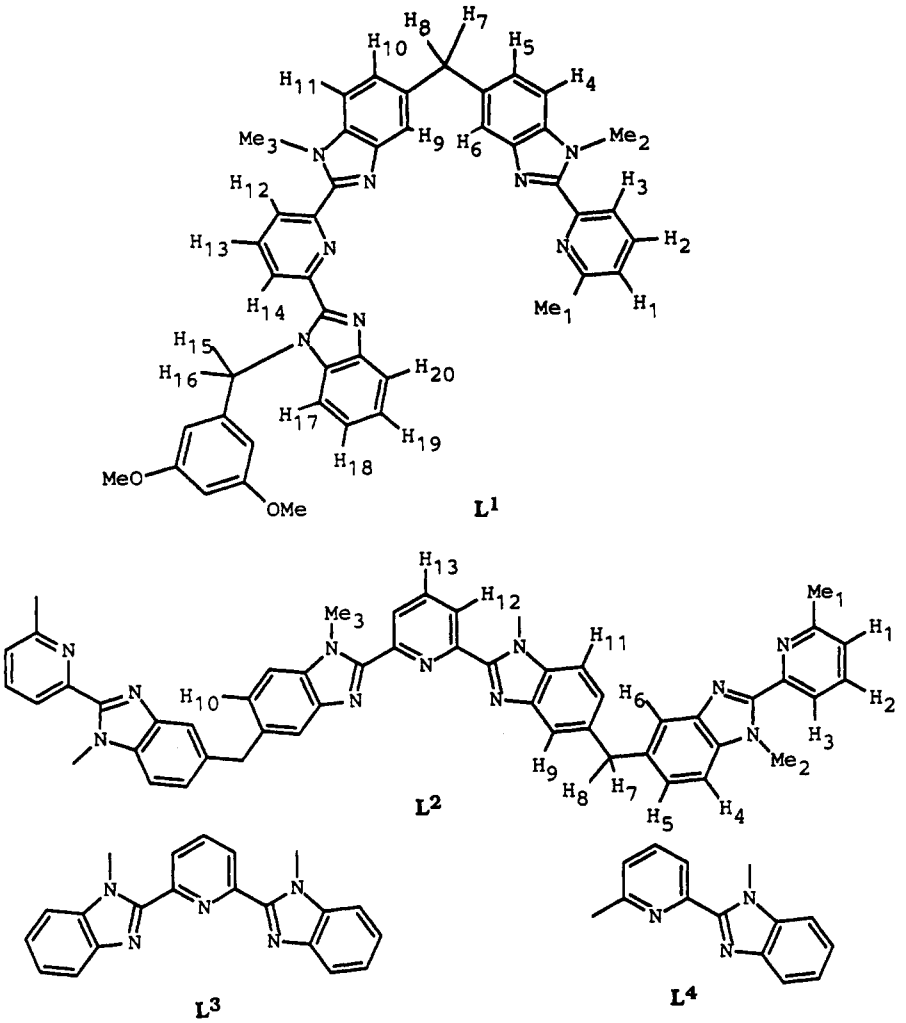

metal ions[9] give polynuclear triple-helical complexes. Following these criteria, Constable and co-workers[17] and later Potts et al.[13] were able to prepare mixed valence dinuclear Cu(II)/Cu(I) double-helical complexes by using quinquepyridine (quinquepy), a pentadentate ligand which acts as a bidentate donor group toward pseudotetrahedral Cu(I) and as a tridentate unit toward pseudo-octahedral Cu(II). Recent extension of this work[18] leads to the synthesis of a double-helical heterodinuclear complex $[CoAg(quinquepy)](PF_6)_3$ where Co(II) occupies the pseudo-octahedral site defined by two terpyridine units, and Ag(I) occupies the remaining pseudotetrahedral site produced by the bipyridine units. However, the lack of spacer between the pyridine rings in oligopyridine ligands allows some ambiguity concerning their binding mode as demonstrated by quinquepyridine (pentadentate or tridentate–bidentate),[17,18] sexipyridine (bistridentate or trisbidentate),[19] and septipyridine (bistridentate, bisbidentate–tridentate, trisbidentate–monodentate).[13] The introduction of suitable spacers[9,11,15,16] between the various coordinating units removes this ambiguity and gives segmental ligands possessing different binding units along the strand. Following this strategy, we have recently synthesized[20] the segmental ligands L^1 (bidentate–tridentate) and L^2 (bidentate–tridentate–bidentate) designed for the self-assembly of heteropolynuclear helical complexes with various metal ions.

In this paper we report the preparation of double-helical homodinuclear $[M_2(L^1)_2]^{4+}$ (M = Zn, Co), heterodinuclear $[M^1M^2(L^1)_2]^{3+}$ (M^1 = Fe, M^2 = Ag, Cu), and heterotrinuclear $[FeAg_2(L^2)_2]^{4+}$ complexes together with the detailed study of the self-assembly processes leading to the selective formation of the final supramolecular complexes in solution.

Experimental Section

Solvents and starting materials were purchased from Fluka AG (Buchs, Switzerland) and used without further purification, unless otherwise stated. The ligands 5-{2′-[6″-(1‴-(3,5-dimethoxybenzyl)-1‴*H*-benzimidazol-2‴-yl)-pyridin-2″-yl]-1′-methyl-1′*H*-benzimidazol-5′-ylmethyl}-1-meth-

(13) Potts, K. T.; Keshavarz-K, M.; Tham, F. S.; Abruna, H. D.; Arana, C. *Inorg. Chem.* **1993**, *32*, 4422–4435. Potts, K. T.; Keshavarz-K, M.; Tham, F. S.; Abruna, H. D.; Arana, C. *Inorg. Chem.* **1993**, *32*, 4436–4449. Potts, K. T.; Keshavarz-K, M.; Tham, F. S.; Abruna, H. D.; Arana, C. *Inorg. Chem.* **1993**, *32*, 4450–4456. Potts, K. T.; Keshavarz-K, M.; Tham, F. S.; Gheysen-Raiford, K. A.; Arana, C.; Abruna, H. D. *Inorg. Chem.* **1993**, *32*, 5477–5484.

(14) Piguet, C.; Bernardinelli, G.; Williams, A. F. *Inorg. Chem.* **1989**, *28*, 2920–2925. Rüttimann, S.; Piguet, C.; Bernardinelli, G.; Bocquet, B.; Williams, A. F. *J. Am. Chem. Soc.* **1992**, *114*, 4230–4237.

(15) Piguet, C.; Bernardinelli, G.; Bocquet, B.; Quattropani, A.; Williams, A. F. *J. Am. Chem. Soc.* **1992**, *114*, 7440–7451. Williams, A. F.; Piguet, C.; Bernardinelli, G. *Angew. Chem., Int. Ed. Engl.* **1991**, *30*, 1490–1492.

(16) Krämer, R.; Lehn, J.-M.; De Cian, A.; Fischer, J. *Angew. Chem., Int. Ed. Engl.* **1993**, *32*, 703–706. Potts, K. T.; Horwitz, C. P.; Fessak, A.; Nash, K. E.; Toscano, P. J. *J. Am. Chem. Soc.* **1993**, *115*, 10444–10445. Goodgame, D. M. L.; Hill, S. P. W.; Williams, D. J. *J. Chem. Soc., Chem. Commun.* **1993**, 1019–1021.

(17) Barley, M.; Constable, E. C.; Corr, S. A.; McQueen, R. S.; Nutkins, J. C.; Ward, M. D.; Drew, M. G. B. *J. Chem. Soc., Dalton Trans.* **1988**, 2655–2662.

(18) Constable, E. C.; Walker, J. V. *J. Chem. Soc., Chem. Commun.* **1992**, 884–886. Constable, E. C.; Edwards, A. J.; Raithby, P. R.; Walker, J. V. *Angew. Chem., Int. Ed. Engl.* **1993**, *32*, 1465–1467.

(19) Constable, E. C.; Ward, M. D.; Tocher, D. A. *J. Chem. Soc., Dalton Trans.* **1991**, 1675–1683.

(20) Piguet, C.; Bocquet, B.; Hopfgartner, G. *Helv. Chim. Acta* **1994**, *77*, 931–942.

yl-2-(6''''-methylpyridin-2''''-yl)-1*H*-benzimidazole (L^1) and 1,1'-dimethyl-2,2'-bis[6-(methylpyridin-2-yl)-5,5'-{pyridine-2,6-diylbis[(1-methyl-1*H*-benzimidazole-2,5-diyl)methylene]}bis[1*H*-benzimidazole] (L^2) were prepared according to previously described multistep syntheses.[20]

Preparation of $[Zn_2(L^1)_2](ClO_4)_4 \cdot 4H_2O$. $Zn(ClO_4)_2 \cdot 6H_2O$ (21 mg, 0.056 mmol) in acetonitrile (3 mL) was added dropwise to a solution of L^1 (40 mg, 0.056 mmol) in acetonitrile/dichloromethane 1:1 (5 mL). The resulting yellow solution was evaporated to dryness under vacuum and dissolved in acetonitrile, and diethyl ether was allowed to diffuse into the solution for 3 days. The white microcrystals were separated by filtration and dried to give 44 mg (0.022 mmol, 78%) of $[Zn_2(L^1)_2](ClO_4)_4 \cdot 4H_2O$: ^{1}H-NMR in CD_3CN 1.92 (6H, s), 3.72 (12H, s), 3.84 (2H, d, J^2 = 15 Hz), 3.92 (2H, d, J^2 = 15 Hz), 4.17 (6H, s), 4.78 (6H, s), 5.77 (2H, s), 5.92 (2H, d, J^2 = 18 Hz), 6.00 (2H, d, J^2 = 18 Hz), 6.26 (4H, d, J^4 = 2 Hz), 6.41 (2H, d, J^3 = 8 Hz), 6.44 (2H, t, J^4 = 2 Hz), 7.08 (2H, t, J^3 = 8 Hz), 7.26 (2H, d, J^3 = 8 Hz), 7.36 (2H, t, J^3 = 8 Hz), 7.38 (2H, d, J^3 = 8 Hz), 7.42 (2H, s), 7.47 (2H, d, J^3 = 8 Hz), 7.51 (2H, d, J^3 = 8 Hz), 7.63 (2H, d, J^3 = 8 Hz), 8.03 (2H, d, J^3 = 8 Hz), 8.15 (2H, t, J^3 = 8 Hz), 8.23 (2H, d, J^3 = 8 Hz), 8.44 (2H, t, J^3 = 8 Hz), 8.50 (2H, d, J^3 = 8 Hz), 8.62 (2H, d, J^3 = 8 Hz). Anal. Calcd for $Zn_2C_{88}H_{76}N_{16}O_{20}Cl_4 \cdot 4H_2O$: Zn, 6.29; C, 52.26; N, 11.08; H, 4.19. Found: Zn, 6.2; C, 52.48; N, 11.11; H, 4.27.

Preparation of $[FeAg(L^1)_2](ClO_4)_3 \cdot 4H_2O$. $Fe(ClO_4)_2 \cdot 6H_2O$ (5.1 mg, 0.014 mmol) in acetonitrile (0.7 mL) was added to a solution of L^1 (20 mg, 0.028 mmol) in acetonitrile/dichloromethane 1:1 (2 mL). The resulting violet solution was stirred for 30 min, and then $AgClO_4 \cdot H_2O$ (3.2 mg, 0.014 mmol) in acetonitrile (0.7 mL) was added. The solution was evaporated to dryness under vacuum and dissolved in acetonitrile, and diethyl ether was allowed to diffuse into the solution for 2 days to give 25 mg (0.0127 mmol, 91%) of $[FeAg(L^1)_2](ClO_4)_3 \cdot 4H_2O$ as violet needles: ^{1}H-NMR in CD_3CN 2.66 (6H, s), 3.37 (12H, s), 3.71 (2H, d, J^2 = 15 Hz), 3.95 (2H, d, J^2 = 15 Hz), 4.12 (6H, s), 4.30 (6H, s), 5.53 (2H, s), 5.75 (4H, d, J^4 = 2 Hz), 5.87 (2H, d, J^2 = 18 Hz), 5.91 (2H, d, J^3 = 8 Hz), 5.98 (2H, d, J^2 = 18 Hz), 6.34 (2H, t, J^4 = 2 Hz), 6.89 (2H, t, J^3 = 8 Hz), 7.06 (2H, d, J^3 = 8 Hz), 7.18 (2H, s), 7.18 (2H, t, J^3 = 8 Hz), 7.20 (2H, d, J^3 = 8 Hz), 7.37 (2H, d, J^3 = 8 Hz), 7.42 (2H, d, J^3 = 8 Hz), 7.45 (2H, d, J^3 = 8 Hz), 7.60 (2H, d, J^3 = 8 Hz), 7.95 (2H, t, J^3 = 8 Hz), 8.14 (2H, d, J^3 = 8 Hz), 8.60 (2H, t, J^3 = 8 Hz), 8.73 (2H, d, J^3 = 8 Hz), 8.91 (2H, d, J^3 = 8 Hz). Anal. Calcd for $FeAgC_{88}H_{76}N_{16}O_{16}Cl_3 \cdot 4H_2O$: Fe, 2.86; Ag, 5.51; C, 54.04; N, 11.46; H, 4.33. Found: Fe, 2.7; Ag, 5.7; C, 54.05; N, 11.42; H, 4.31.

Preparation of $[FeAg_2(L^2)_2](ClO_4)_4 \cdot 4H_2O$. A similar procedure was followed from L^2 with $Fe(ClO_4)_2 \cdot 6H_2O$ and $AgClO_4 \cdot H_2O$ to give 87% of $[FeAg_2(L^2)_2](ClO_4)_4 \cdot 4H_2O$ as violet pellets which were crystallized from acetonitrile/methanol. ^{1}H-NMR in CD_3CN: 2.73 (12H, s), 3.63 (12H, s), 3.80 (8H, s), 4.36 (12H, s), 5.24 (4H, s), 6.87 (4H, d.d., J^3 = 8 Hz, J^4 = 1 Hz), 7.19 (4H, d, J^3 = 8 Hz), 7.24 (4H, d.d., J^3 = 8 Hz, J^4 = 1 Hz), 7.54 (4H, d, J^3 = 8 Hz), 7.60 (4H, s), 7.68 (4H, d, J^3 = 8 Hz), 8.02 (4H, d, J^3 = 8 Hz), 8.19 (4H, t, J^3 = 8 Hz), 8.28 (2H, t, J^3 = 8 Hz), 8.29 (4H, d, J^3 = 8 Hz). Anal. Calcd for $FeAg_2C_{102}H_{80}N_{22}O_{16}Cl_4 \cdot 4H_2O$: Fe, 2.37; Ag, 9.14; C, 51.88; N, 13.05; H, 4.01. Found: Fe, 2.4; Ag, 9.2; C, 52.15; N, 13.07; H, 4.02.

Caution! Perchlorate salts with organic ligands are potentially explosive and should be handled with the necessary precautions.[21]

Spectroscopic and Analytical Measurements. IR spectra were obtained from KBr pellets with a Perkin Elmer IR 883 spectrometer. Electronic spectra in the UV–visible range were recorded at 20 °C in acetonitrile solution with a Perkin-Elmer Lambda 5 spectrometer using quartz cells of 1, 0.1, and 0.01 cm path length. Spectrophotometric titrations were performed with a Perkin-Elmer Lambda 5 spectrophotometer connected to an external computer. In a typical experiment, 50 mL of ligand (L^1, L^2) in acetonitrile (10^{-4} M) were titrated with a 2.0×10^{-3} M solution of the perchlorate salt of the appropriate metal ion in acetonitrile. After each addition of 0.20 mL, the absorbances at 10 different wavelengths were recorded using a 0.1 cm quartz cell and transferred to the computer. Plots of extinction as a function of the metal/ligand ratio gave a first indication of the number and stoichiometry of the complexes formed: factor analysis[22] was then applied to the data to confirm the number of different absorbing species. Finally, a model for the distribution of species was fitted with a nonlinear least-squares algorithm to give stability constants as previously described.[15] Pneumatically-assisted electrospray (ion spray) mass spectra were recorded on an API III tandem mass spectrometer (PE Sciex) by infusion at 4–10 μL/min. The spectra were recorded under low up-front declustering or collision induced dissociation (CID) conditions,[23] typically ΔV = 0–30 V between the orifice (OR) and the first quadrupole of the Sciex. Determination of the total charge (z) of the complexes was made by using the isotopic pattern ($z \leq 3$) or adduct ions with perchlorate anions ($z > 3$).[24] ES-MS titrations were performed in the same conditions as described for the spectrophotometric titrations, ES-MS spectra being recorded after each addition of the metal solution. ^{1}H-NMR and ^{13}C-NMR spectra were recorded on Varian Gemini 300 spectrometer. Chemical shifts are given in ppm w.r.t. TMS; abbreviations: s, singlet; d, doublet; d.d, doublet of doublet; t, triplet; m, multiplet. Cyclic voltammograms were recorded using a Cypress System potentiostat connected to a personnal computer ATM A386SX. A three-electrode system consisting of a stationary Pt disk working electrode, a Pt counter electrode, and a nonaqueous Ag/Ag^+ reference electrode was used. NBu_4PF_6 (0.1 M in CH_3CN) served as inert electrolyte, and CH_3CN was distilled from P_2O_5 and then passed through an Alox column (activity I). The reference potential ($E°$ = 0.37 (V) vs SCE) was standardized against $[Ru(bipy)_3](ClO_4)_2$.[25] The scan speed used was 100 mV/s, and voltammograms were analyzed according to established procedures.[25] Elemental analyses were performed by Dr. H. Eder of the Microchemical Laboratory of the University of Geneva. Metal contents were determined by Atomic Absorption (Pye Unicam SP9) after acidic oxidative mineralization of the complexes.

Results

The ligands L^1 and L^2 possess two different binding units separated by diphenylmethane spacers which favor the formation of polynuclear helical complexes.[9,15] The tridentate donor group, an analogue of 2,2':6',2''-terpyridine[26] and L^3,[27] is designed for the formation of D_{2d}-symmetrical $[ML_2]^{n+}$ complexes with octahedral metal ions,[27,28] while the bidentate unit, an analogue of 6-methyl-2,2'-bipyridine and L^4,[15] favors the formation of C_2-symmetrical $[ML_2]^{n+}$ complexes with tetrahedral metal ions.[11–13,15] We thus expect the formation of dinuclear or trinuclear double-helical complexes when respectively L^1 or L^2 reacts with mixtures of tetrahedral and octahedral metal ions. Our strategy is based on the following approach: (i) study of the homopolynuclear complexes formed by L^1 and L^2 with octahedral and tetrahedral metal ions and (ii) characterization of the heteropolynuclear complexes with L^1 and L^2. In order to limit the amount of ligand required for the studies, we have used a new approach for the characterization of the supramolecular complexes based on an efficient combination of electrospray mass spectrometry (ES-MS),[24] spectrophotometric,[9,15] and ^{1}H-NMR titrations in solution followed by isolation of the complexes as their perchlorate salts.

Homodinuclear Complexes with L^1. Fe(II) forms mainly diamagnetic low-spin pseudo-octahedral complexes with diimine and triimine ligands, and only very few tetrahedral complexes are known.[29] ES-MS titration of L^1 by $Fe(ClO_4)_2 \cdot 6H_2O$ in acetonitrile shows the exclusive formation of $[Fe(L^1)_2]^{2+}$ (m/z = 739, Table 1) for Fe/L^1 ratio in the range 0.1–0.5. Even in excess of Fe(II) (Fe/$L^1 \geq 1$), we still observe $[Fe(L^1)_2]^{2+}$ as the major peak together with small peaks corresponding to $[Fe_2(L^1)_2]^{4+}$ (m/z = 383) and its adduct ions with perchlorate anions $[Fe_2(L^1)_2(ClO_4)]^{3+}$ and $[Fe_2(L^1)_2(ClO_4)_2]^{2+}$ (Table 1).[24] Spectrophotometric titrations in the same conditions confirm these results, and we observe a sharp end point for a Fe(II):ligand ratio

(21) Wolsey, W. C. *J. Chem. Educ.* **1978**, *55*, A355.
(22) Malinowski, E. R.; Howery, D. G. *Factor Analysis in Chemistry*; J. Wiley: New York, Chichester, Brisbane, and Toronto, 1980.
(23) Hopfgartner, G.; Bean, K.; Wachs, T.; Henion, J. D. *Anal. Chem.* **1993**, *65*, 439–446.
(24) Hopfgartner, G.; Piguet, C.; Henion, J. D.; Williams, A. F. *Helv. Chim. Acta* **1993**, *76*, 1759–1766. Hopfgartner, G.; Piguet, C.; Henion; J. D. *J. Am. Soc. Mass Spec.*, in press.
(25) Bard, A. J.; Faulkner, L. R. *Electrochemical Methods, Fundamentals and Application*; J. Wiley: New York, Chichester, Brisbane, Toronto, Singapore, 1980.
(26) Piguet, C.; Bochet, C. G.; Williams, A. F. *Helv. Chim. Acta* **1993**, *76*, 372–384.
(27) Rüttimann, S.; Moreau, C. M.; Williams, A. F.; Bernardinelli, G.; Addison, A. W. *Polyhedron* **1992**, *11*, 635–646.
(28) Piguet, C.; Bocquet, B.; Müller, E.; Williams, A. F. *Helv. Chim. Acta* **1989**, *72*, 323–337.
(29) Cotton, F. A.; Wilkinson, G. *Advanced Inorganic Chemistry*, 4th ed.; John Wiley & Sons: New York, Chichester, Brisbane, Toronto, 1980.

Table 1. Molecular Peaks of Complexes and Adduct Ions Observed by ES-MS for the Titration of Ligands L^1 and L^2 with Various Metal Ions

ligand	metal	cations	m/z[a]
L^1	Fe(II)	$[Fe(L^1)_2]^{2+}$	739
		$[Fe_2(L^1)_2]^{4+}$	383
		$[Fe_2(L^1)_2(ClO_4)]^{3+}$	544
		$[Fe_2(L^1)_2(ClO_4)_2]^{2+}$	867
L^1	Co(II)	$[Co(L^1)_3]^{2+}$	1095.5
		$[Co(L^1)_2]^{2+}$	740
		$[Co_2(L^1)_2]^{4+}$	385
		$[Co_2(L^1)_2(ClO_4)]^{3+}$	546
		$[Co_2(L^1)_2(ClO_4)_2]^{2+}$	869
L^1	Zn(II)	$[Zn(L^1)_3]^{2+}$	1099
		$[Zn(L^1)_2]^{2+}$	743
		$[Zn_2(L^1)_2]^{4+}$	388
		$[Zn_2(L^1)_2(ClO_4)]^{3+}$	551
		$[Zn_2(L^1)_2(ClO_4)_2]^{2+}$	875
L^1	Ag(I)	$[Ag_2(L^1)_2]^{2+}$	817
L^1	Fe(II)/Ag(I)	$[Fe(L^1)_2]^{2+}$	739
		$[FeAg(L^1)_2]^{3+}$	528
		$[FeAg(L^1)_2(ClO_4)]^{2+}$	841
L^2	Fe(II)	$[Fe(L^2)_2]^{2+}$	838
		$[Fe_2(L^2)_2]^{4+}$	433
		$[Fe_2(L^2)_2(ClO_4)]^{3+}$	610
		$[Fe_2(L^2)_2(ClO_4)_2]^{2+}$	965
L^2	Ag(I)	$[Ag(L^2)_2]^{+}$	1727
		$[Ag_2(L^2)_2]^{2+}$	918
		$[Ag_3(L^2)_2]^{3+}$	648
		$[Ag_4(L^2)_2]^{4+}$	513
		$[Ag_4(L^2)_2(ClO_4)]^{3+}$	715
L^2	Fe(II)/Ag(I)	$[Fe(L^2)_2]^{2+}$	838
		$[FeAg(L^2)_2]^{3+}$	595
		$[FeAg(L^2)_2(ClO_4)]^{2+}$	941
		$[FeAg_2(L^2)_2]^{4+}$	473
		$[FeAg_2(L^2)_2(ClO_4)]^{3+}$	664
		$[FeAg_2(L^2)_2(ClO_4)_2]^{2+}$	1045

[a] Nominal m/z values given for the maximum of the peak.

of 0.5 followed by a weak evolution of the electronic spectra leading to a second less pronounced end point around $Fe/L^1 = 1$. Factor analysis[22] suggests the existence of two absorbing complexes, and the spectrophotometric data can be satisfactorily fitted with the equilibria 1, 2, and $\log(\beta_{12}) = 14.0(7)$ (M = Fe), but the similarity of the spectra of the two complexes prevents a precise determination of $\log(\beta_{22})$[30] which can be only estimated for $[Fe_2(L^1)_2]^{4+}$ to be around $\log(\beta_{22}) = 17$.

$$M^{2+} + 2L^1 \leftrightarrow [M(L^1)_2]^{2+} \qquad \log(\beta_{12}) \qquad (1)$$

$$2M^{2+} + 2L^1 \leftrightarrow [M_2(L^1)_2]^{4+} \qquad \log(\beta_{22}) \qquad (2)$$

The electronic spectrum of $[Fe(L^1)_2]^{2+}$ displays the typical intraligand $\pi_1 \rightarrow \pi^*$ transitions[26,27] and the strong metal-to-ligand charge transfer band (Fe(II) $\rightarrow \pi^*$ MLCT)[26,27,31] centered at 17 270 cm^{-1} (Table 2) which are observed when Fe(II) is pseudo-octahedrally coordinated by two tridentate units as in $[Fe(L^3)_2]^{2+}$.

The ^{1}H-NMR spectrum of the free ligand L^1 is rather complicated, but 2D-COSY and 2D-NOESY spectra allow a complete assignment of the 24 signals (Table 3). 2D-NOESY measurements show a significant cross peak between the methylene protons H_{15}, H_{16}, and Me_3 but no cross peaks between H_{15}, H_{16}, and H_{14} or between Me_2 and H_3 which implies that the pyridine and benzimidazole rings within the tridentate and the bidentate units adopt transoid conformations as previously reported for many free oligopyridines.[12,32] Upon coordination to Fe(II) to give $[Fe(L^1)_2]^{2+}$, the ^{1}H-NMR signals of the bidentate

Table 2. Electronic Spectral Data for the Ligands L^1, L^2 in $CHCl_3$, and Their Complexes in CH_3CN[a] and Electrochemical Reduction Potentials in CH_3CN[b] at 20 °C

compd	$\pi \rightarrow \pi^*$	MLCT	$E_{1/2}$	$E_{pa} - E_{pc}$
L^1	34 480(34 280 sh)		−1.98	120[c]
	31 545(52 490)			
L^2	31 350(82 620)			
$[Zn_2(L^1)_2]^{4+}$	31 410(85 900)			
	28 570(65 950 sh)			
	27 170(44 010 sh)			
$[Fe(L^1)_2]^{2+}$	35 210(64 000 sh)	17 270(9820)	0.83[c]	70
	31 645(95 800)		−1.05[d]	70
	28 170(50 160)		−1.46[d]	80
	26 810(56 470)			
$[Fe(L^2)_2]^{2+}$	31 750(14 2570)	17 180(8730)	0.75[c]	80
	27 780(48 320)		−1.11[d]	70
	26 525(59 270)		−1.57[d]	80
$[FeAg(L^1)_2]^{3+}$	35 710(53 100 sh)	17 240(9000)	0.84[c]	70
	31 650(83 770)		0.11[e]	240
	28 090(48 000)		−1.06[d]	70
	26 740(55 610)		−1.47[d]	70
$[FeAg_2(L^2)_2]^{4+}$	31 150(14 7020)	16 950(10 560)	0.73[c]	110
	28 090(41 250)		−0.07[e]	440
	26 525(50 390)		−1.11[d]	60
			−1.57[d]	90

[a] Energies are given for the maximum of the band envelope in cm^{-1} and ϵ (in parentheses) in M^{-1} cm^{-1}; sh = shoulder. [b] Electrochemical potentials are given in V vs SCE and $E_{pa} - E_{pc}$ in [mV]. Estimated error on $E_{1/2}$ is ±0.01 V. [c] Reduction centered on the metal. [d] Reduction centered on the ligand. [e] $E_{p/2}$ in V vs SCE for irreversible Ag(I)/Ag(0) reduction process.

units are only weakly altered, but the signals of the tridentate unit are significantly modified. The methylene protons H_{15} and H_{16} become diastereotopic and give an AB spin system as a result of the loss of the symmetry plane in the complex,[14] and the pyridine proton H_{13} is shifted toward lower field ($\Delta\delta = 0.51$ ppm) which is typical for N-coordination of the pyridine ring.[26,33] The protons H_9 and H_{20} are significantly shielded in $[Fe(L^1)_2]^{2+}$ ($\Delta\delta = 2.15$ and 1.93 ppm, respectively) which is typical for pseudo-octahedral coordination of the tridentate units around Fe(II) which puts these protons above the pyridine ring of the other ligand, as previously described for $[Fe(L^3)_2]^{2+}$ [26] and $[Fe(terpy)_2]^{2+}$.[34] New cross peaks between Me_3 and H_{12} and between H_{15}, H_{16}, and H_{14} are observed in the NOESY spectrum of $[Fe(L^1)_2]^{2+}$ which indicate that the tridentate binding units of L^1 adopts a cis–cis conformation in the complex. The ^{1}H-NMR results confirm the electronic spectrum and unambigously establish that $[Fe(L^1)_2]^{2+}$ adopts the head-to-head C_2-symmetrical structure I where Fe(II) is pseudo-octahedrally coordinated by the two tridentate sites (Figure 1).

Compared to Fe(II), Co(II), and Zn(II) display less pronounced stereochemical preferences for pseudo-octahedral coordination and both octahedral and tetrahedral complexes are commonly found with diimine and triimine ligands.[29] ES-MS titrations of L^1 with $Zn(ClO_4)_2 \cdot 6H_2O$ or $Co(ClO_4)_2 \cdot 6H_2O$ in acetonitrile give very similar results and show the formation of $[M(L^1)_2]^{2+}$ (M = Co, Zn) as the major species in solution for metal:ligand ratio between 0.1 and 0.7 as previously observed for Fe(II). However, in large excess of ligand (M:L = 0.1–0.2), a very weak peak corresponding to traces of $[M(L^1)_3]^{2+}$ is observed at $m/z = 1095.5$ (Co) and 1099 (Zn) which strongly suggests that the bidentate units have only a weak tendency to form octahedral complexes with Co(II) or Zn(II) as previously reported for the ligand L^4 with Co(II).[15,24] In excess of M(II) (M(II)/L ≥ 1), we still observe $[M(L^1)_2]^{2+}$ together with significant peaks corresponding to $[M_2(L^1)_2]^{4+}$ (and their adduct ions $[M_2(L^1)_2(ClO_4)]^{3+}$ and $[M_2(L^1)_2(ClO_4)_2]^{2+}$. $[M_2(L^1)_2]^{4+}$ becomes the major species for

(30) Piguet, C.; Bünzli, J.-C G.; Bernardinelli, G.; Williams, A. F. *Inorg. Chem.* **1993**, *32*, 4139–4149.
(31) Krumholz, P. *Struct. Bonding* **1971**, *9*, 139–174.
(32) Nakamoto, K. *J. Phys. Chem.* **1960**, *64*, 1420–1425. Constable, E. C.; Elder, S. M.; Walker, J. V.; Wood, P. P.; Tocher, D. A. *J. Chem. Soc., Chem. Commun.* **1992**, 229–231.
(33) Lavallee, D. K.; Baughman, M. D.; Phillips, M. P. *J. Am. Chem. Soc.* **1977**, *99*, 718–724.
(34) Elsbernd, H.; Beattie, J. K. *J. Inorg. Nucl. Chem.* **1972**, *34*, 771–774.

Table 3. ^{1}H-NMR Shifts (with Respect to TMS) for Ligands L^1, L^2 in $CDCl_3$, and Their Complexes in CD_3CN at 20 °C

Bidentate Binding Unit

compd	Me_1	Me_2	H_1	H_2	H_3	H_4	H_5	H_6	H_7,H_8
L^1	2.61	4.22	7.20	7.75	8.08	7.2–7.4	7.2–7.4	7.58	4.24
$[Zn(L^1)_2]^{2+}$	2.69	4.31	7.36	7.86	8.16	7.23	6.90	7.15	3.86, 3.93
$[Zn_2(L^1)_2]^{4+}$	1.92	4.78	7.38	8.15	8.62	8.03	7.51	7.42	3.84, 3.92
$[Fe(L^1)_2]^{2+}$	2.68	4.40	7.29	7.85	8.23	7.26	6.90	7.60	3.77, 3.90
$[FeAg(L^1)_2]^{3+}$	2.66	4.30	7.45	7.95	8.14	7.60	7.06	7.18	3.71, 3.91
L^2	2.63	4.25	7.18	7.72	8.16	7.35	7.26	7.74	4.30
$[Fe(L^2)_2]^{2+}$	2.66	4.33	7.30	7.83	8.20	7.40	7.13	7.22	3.84
$[FeAg_2(L^2)_2]^{4+}$	2.73	4.36	7.68	8.19	8.29	7.54	7.24	7.60	3.80

Tridentate Binding Unit

compd	Me_3	H_9	H_{10}	H_{11}	H_{12}	H_{13}	H_{14}	$H_{15,16}$	H_{17}	H_{18}	H_{19}	H_{20}
L^1	3.81	7.62	7.2–7.4	7.2–7.4	8.40	8.07	8.28	5.99	7.2–7.4	7.2–7.4	7.2–7.4	7.70
$[Zn(L^1)_2]^{2+}$	4.14	5.87	7.28	7.43	8.29	8.40	8.20	5.86	7.44	7.27	6.97	6.26
$[Zn_2(L^1)_2]^{4+}$	4.17	5.77	7.26	7.47	8.50	8.44	8.23	5.92 6.00	7.63	7.36	7.08	6.41
$[Fe(L^1)_2]^{2+}$	4.14	5.47	7.10	7.40	8.44	8.58	8.44	5.83	7.1–7.6	7.1–7.6	6.90	5.77
$[FeAg(L^1)_2]^{3+}$	4.12	5.33	7.20	7.37	8.73	8.60	8.91	5.87 5.98	7.42	7.18	6.89	5.91
L^2	4.20	7.71	7.25	7.32	8.37	8.01						
$[Fe(L^2)_2]^{2+}$	4.06	5.53	6.91	7.23	8.48	8.42						
$[FeAg_2(L^2)_2]^{4+}$	3.63	5.24	6.87	7.19	8.02	8.28						

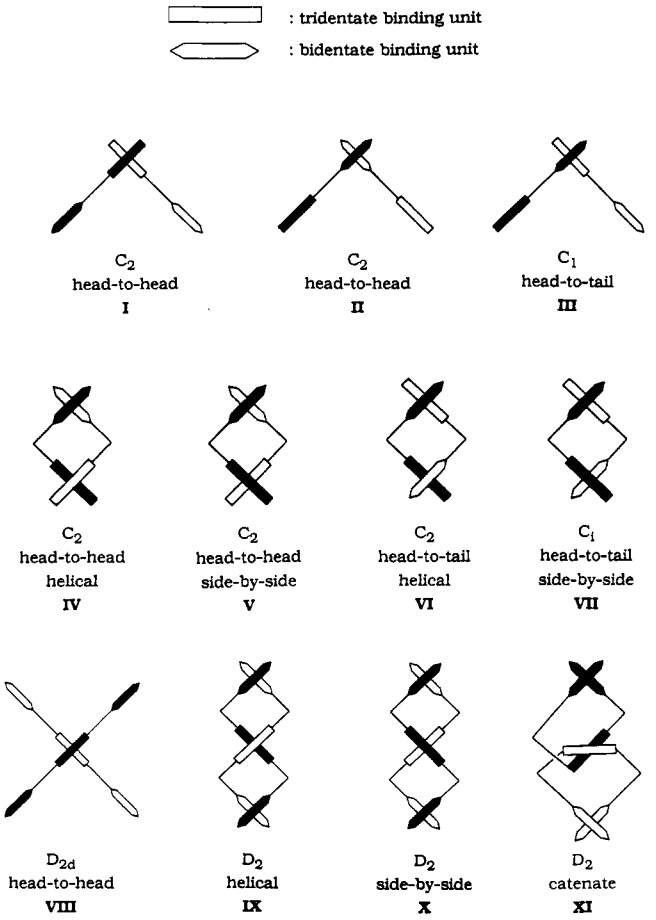

Figure 1. Possible structures for complexes $[M(L^1)_2]^{n+}$ (I–III), $[M_2(L^1)_2]^{n+}$ (IV–VII), $[M(L^2)_2]^{n+}$ (VIII), and $[M_3(L^2)_2]^{n+}$ (IX–XI); M = Fe, Co, Zn, Cu, and Ag.

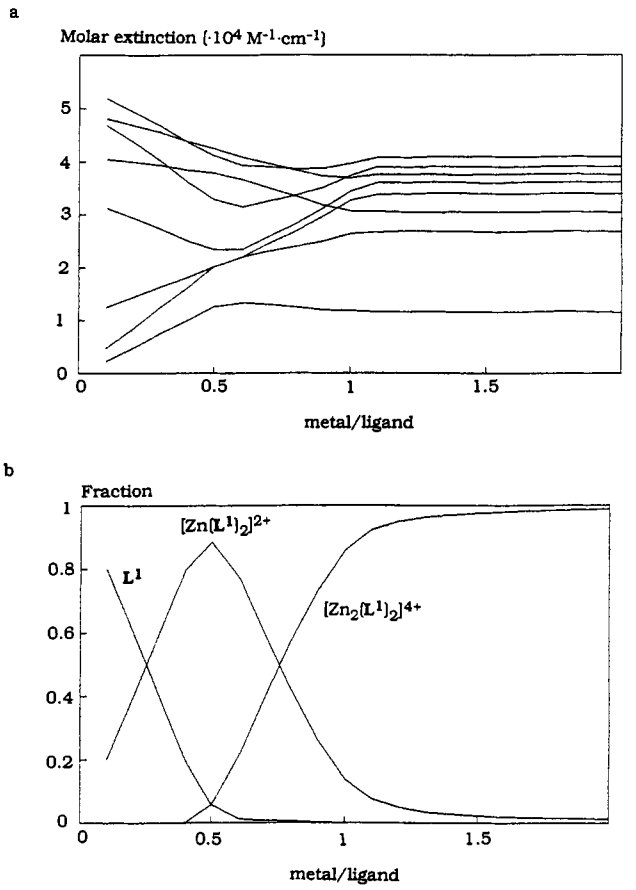

Figure 2. (a) Variation of observed molar extinction and (b) corresponding speciation of ligand for the spectrophotometric titration of L^1 with $Zn(ClO_4)_2{\cdot}6H_2O$ in CH_3CN at 20 °C (total ligand concentration: 10^{-4} M).

M(II)/L ≥ 1.5 (M = Co, Zn). Spectrophotometric titrations in the range M:L^1 = 0.2–2.5 confirm this behavior and display two sharp end points for metal:ligand ratio of 0.5:1.0 (Figure 2). Factor analysis[22] implies the existence of only two absorbing complexes, and the spectrophotometric data can be satisfactorily fitted with equilibria 1, 2, and $\log(\beta_{12})$ = 14.3(8), $\log(\beta_{22})$ = 20.3(8) for M = Co and $\log(\beta_{12})$ = 13.9(3), $\log(\beta_{22})$ = 19.8(3) for M = Zn(II). Convergence was obtained with a root-mean-square (RMS) difference between observed and calculated absorbance of 0.005 absorbance units or less.

Detailed ^{1}H-NMR studies (COSY, NOESY, and NOEDIF) of the diamagnetic zinc(II) complexes in CD_3CN show that $[Zn(L^1)_2]^{2+}$ adopts a C_2-symmetrical structure of type **I** very similar to that found for $[Fe(L^1)_2]^{2+}$ with the two tridentate units coordinated to Zn(II) (Table 3). The ^{1}H-NMR spectrum of $[Zn_2(L^1)_2]^{4+}$ displays 26 signals corresponding to a symmetrical

Chart 2

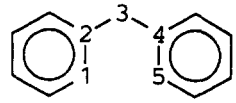

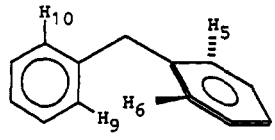

IV

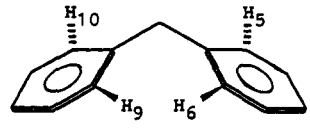

V

arrangement of the two ligands L^1 around the metal ions. The two methylene groups H_7 and H_8 and H_{15} and H_{16} give diastereotopic protons[14] but do not allow one to distinguish between the possible structures IV–VII (Figure 1). The 2D-NOESY spectrum confirms that both bidentate and tridentate binding units display cisoïd conformations as a result of their coordination to Zn(II) (cross peaks between Me_3 and H_{12}, H_{15}, H_{16}, and H_{14}, and Me_2 and H_3, Figure 3), but comparison of the ^{1}H-NMR spectra of $[Zn(L^1)_2]^{2+}$ and $[Zn_2(L^1)_2]^{4+}$ shows that except for H_9 (upfield shift = 0.10 ppm), which lies near the methylene spacer, the signals of the protons bound to the tridentate units are not significantly modified by the complexation of the second Zn(II). On the other hand, the signal of the protons bound to the bidentate units are significantly modified when going from $[Zn(L^1)_2]^{2+}$ to $[Zn_2(L^1)_2]^{4+}$: *(i) downfield shifts of the pyridine protons* H_2 *and* H_3 ($\Delta\delta$ = 0.29 and 0.46 ppm, respectively) typical of N-coordination of the pyridine ring[26,33] and (ii) upfield shift of Me_1 ($\Delta\delta$ = 0.77 ppm) typical of pseudotetrahedral arrangements of the bidentate units around a metal ion as similarly reported for $[Cu(L^4)_2]^{+}$ [15] and for 6,6′-substituted-2,2′-bipyridines.[11] These observations are only compatible with C_2-symmetrical head-to-head structures IV (helical) and V (side-by-side) where one Zn(II) is pseudo-octahedrally coordinated by two tridentate units and the second Zn(II) pseudo-tetrahedrally coordinated by the two remaining bidentate units.

The discrimination between structures IV and V requires detailed measurements of the NOE effects experienced by the protons situated near the spacer (H_5, H_6, H_9, and H_{10}). Consideration of molecular models and molecular mechanics calculations using CHARMM V23.f2 program[35] (vide infra) show that the geometries of the aromatic rings connected by the methylene spacer are significantly different for helical (IV) and side-by-side (V) complexes (Chart 2). A helical structure requires that the torsion angle C_1–C_2–C_3–C_4 is around 0°, while the second torsion angle C_2–C_3–C_4–C_5 lies near 90° as depicted in Chart 2. H_9 is located between H_5 and H_6 (contact distance 3.0–3.3 Å depending on the structural parameters used for the diphenylmethane spacer)[9,15] in the shielding region of the second benzimidazole ring, and we expect both upfield shift of H_9 and two NOE effects of comparable intensities between H_9–H_5 and H_9–H_6. On the other hand, side-by-side complex V requires that both torsions angles lie around 90° producing a geometrical arrangement of the hydrogen atoms where we expect no significant upfield shift of H_9 and two NOE signals between H_6–H_9 and H_5–H_{10} (2.8–3.0 Å) since NOE effects are limited to short distances for small molecules.[36] Selected ^{1}H-NMR spectra and NOEDIF and 2D-NOESY measurements are shown in Figure 3, and they unambiguously establish that $[Zn_2(L^1)_2]^{4+}$ adopts the helical structure IV in acetonitrile (H_9 shifted upfield by 0.1 ppm, NOE enhancement effects between H_9–H_5 and H_9–H_6). This complex has been isolated as its perchlorate salt by diffusion of ether into an acetonitrile solution to give white microcrystals whose elemental analyses and IR spectrum correspond to $[Zn_2(L^1)_2](ClO_4)_4{\cdot}4H_2O$. ES-MS, ^{1}H-NMR, and UV–vis spectra are identical to those measured for the complex $[Zn_2(L^1)_2]^{4+}$ prepared in situ, but we were unable to obtain crystals suitable for X-ray diffraction studies.

ES-MS titrations of L^1 with $Ag(ClO_4){\cdot}H_2O$ or $Cu(CH_3CN)_4(ClO_4)$ in acetonitrile indicate the exclusive formation of $[Ag_2(L^1)_2]^{2+}$ and $[Cu_2(L^1)_2]^{2+}$ for metal:ligand ratio between 0.2 and 2.0. Spectrophotometric titrations of L^1 by $Ag(ClO_4){\cdot}H_2O$ for Ag:ligand ratio of 0.1:2.8 confirm this statement and show a sharp end point for Ag/L^1 = 1.0. Factor analysis[22] indicates the formation of only one absorbing complex and the data can be satisfactorily fitted with the single equilibrium 2 (M = Ag) and $\log(\beta_{22})$ = 14.5(5) (RMS = 0.002); a stability constant similar to that obtained for $[Ag_2(L^3)_2]^{2+}$ by spectrophotometry (14.5(5)) and potentiometry (14.6(1)) in acetonitrile.[38] As a result of the complicated exchange processes observed for these complexes in CD_3CN,[14] no detailed ^{1}H-NMR structural studies were carried out.

Heterodinuclear Complexes with L^1. The formation of heteronuclear complexes by L^1 was studied with various mixtures of octahedral metal ions (Fe(II), Co(II), and Ni(II)) and tetrahedral metal ions (Cu(I), Ag(I)). For spectroscopic reasons, we have focused our attention on the Fe(II)/Ag(I) pair which gives stable diamagnetic heteronuclear complexes. ES-MS titrations of L^1 with an equimolar mixture of $Fe(ClO_4)_2{\cdot}6H_2O$ and $AgClO_4{\cdot}H_2O$ in acetonitrile shows the formation $[Fe(L^1)_2]^{2+}$ as the single complex observed for total metal (M_{tot} = Fe(II) + Ag(I)) to ligand ratio between 0.1 and 1.0. In excess of metal ions (M_{tot}:L^1 > 1), we observe the formation of the heteronuclear complex $[FeAg(L^1)_2]^{3+}$ (m/z = 528) and its adduct ion $[FeAg(L^1)_2(ClO_4)]^{2+}$ at m/z = 841 which become the major peaks for M_{tot}:L^1 ≥ 2 (Figure 4). These results indicate that the affinity of Ag(I) for $[Fe(L^1)_2]^{2+}$ is rather low at 10^{-4} M as a result of steric constraints (vide infra), but it is worth noting that no complexes other than $[Fe(L^1)_2]^{2+}$ and $[FeAg(L^1)_2]^{3+}$ were detected during the titration (M_{tot}:L^1 between 0.1 and 2).

Spectrophotometric titrations of L^1 with an equimolar mixture of $Fe(ClO_4)_2{\cdot}6H_2O$ and $AgClO_4{\cdot}H_2O$ in the same conditions as described for ES-MS show a sharp end point for a total metal:L^1 ratio of 1.0. Factor analysis[22] implies the existence of two absorbing complexes $[Fe(L^1)_2]^{2+}$ and $[FeAg(L^1)_2]^{3+}$ which is confirmed by the titration of $[Fe(L^1)_2]^{2+}$ (prepared in situ) with $AgClO_4{\cdot}H_2O$ where only one new absorbing species is observed for Ag^+:$[Fe(L^1)_2]^{2+}$ = 1.0. Spectrophotometric data can be satisfactorily fitted with the following equilibrium (RMS = 0.001):

$$[Fe(L^1)_2]^{2+} + Ag^+ \leftrightarrow [FeAg(L^1)_2]^{3+} \qquad \log(\beta) = 4.0(3) \tag{3}$$

Combination of eqs 1 and 3 gives an estimated stability constant of $\log(\beta)$ = 18 for $[FeAg(L^1)_2]^{3+}$, but the low affinity of Ag^+ for $[Fe(L^1)_2]^{2+}$ implies that significant decomplexation occurs at low concentration and only 27% of heteronuclear complex $[FeAg(L^1)_2]^{3+}$ is formed at the end point under the titration conditions in good qualitative agreement with the ES-MS results. The

(35) Brooks, B. R.; Bruccoleri, R. E.; Olafson, B. D.; States, D. J.; Swaminathan, S.; Karplus, M. *J. Comput. Chem.* **1983**, *4*, 187–217.

(36) Friebolin, H. *Basic One and Two-dimensional NMR Spectroscopy*; VCH: Weinheim, 1991; pp 251–261.

(37) Dobson, J. F.; Green, B. E.; Healy, P. C.; Kennard, C. H. L.; Pakawatchai, C.; White, A. H. *Aust. J. Chem.* **1984**, *37*, 649–659. Goodvin, K. V.; McMillin, D. R.; Robinson, W. R. *Inorg. Chem.* **1986**, *25*, 2033–2036.

(38) Petoud, S.; Bünzli, J.-C. G.; Piguet, C., unpublished results.

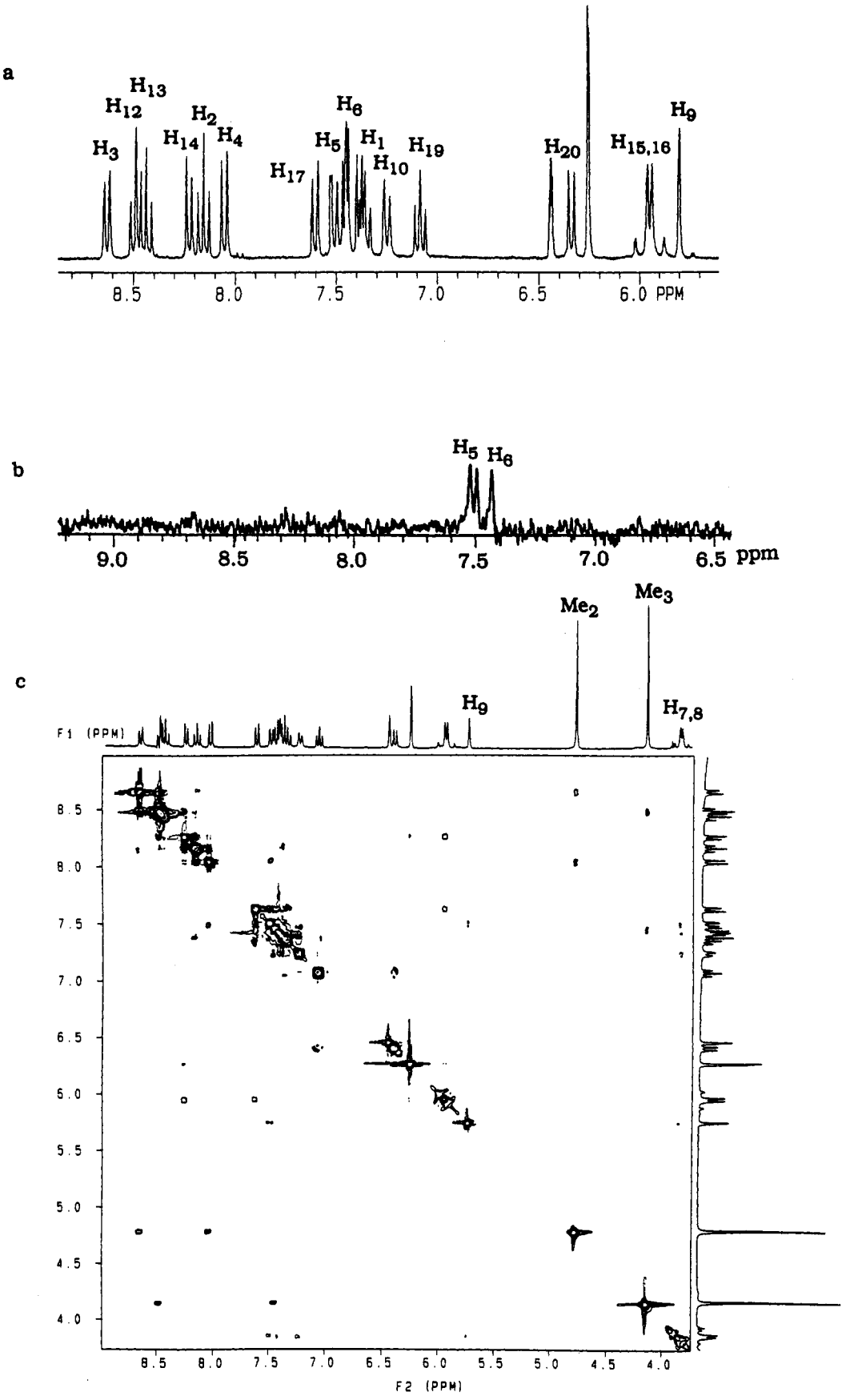

Figure 3. (a) ^{1}H-NMR spectrum, (b) NOEDIF spectrum upon irradiation of H_9, and (c) 2D-NOESY spectrum of 7×10^{-3} M $[Zn_2(L^1)_2]^{4+}$ in CD_3CN at 20 °C.

electronic spectrum of $[FeAg(L^1)_2]^{3+}$ (10^{-3} M in acetonitrile, decomplexation ≈ 25%) is qualitatively similar to that observed for $[Fe(L^1)_2]^{2+}$ (Table 2, Figure 7) showing the splitting of the intraligand $\pi_1 \rightarrow \pi^*$ transitions[26,27] and the strong metal-to-ligand charge transfer band (Fe(II) → π^* MLCT)[26,27,31] centered at 17 240 cm^{-1} typical of Fe(II) pseudo-octahedrally coordinated

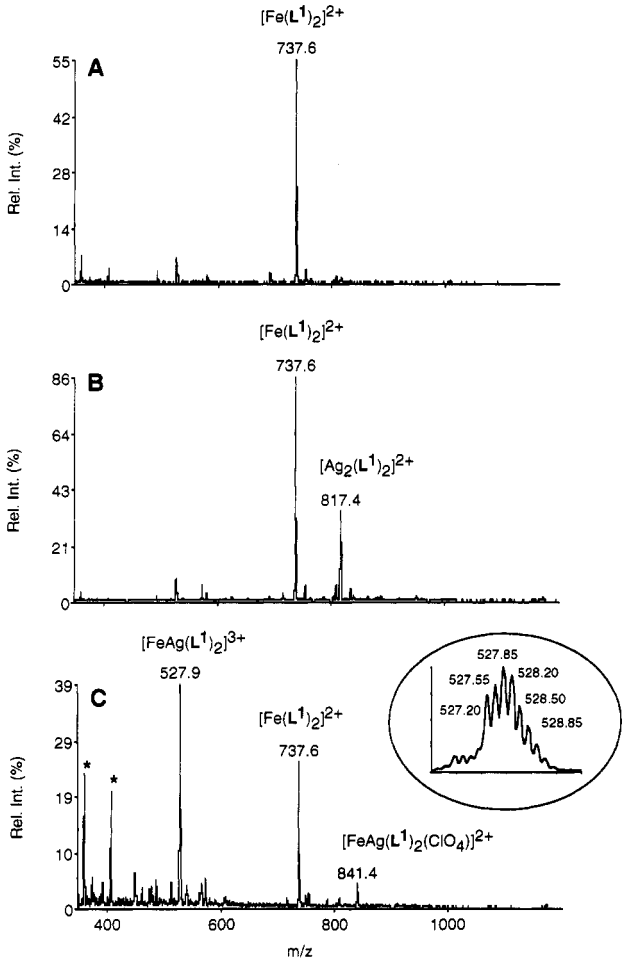

Figure 4. ES-MS spectra ($\Delta V = 0$ V) for the titration of L^1 with Fe(II)/Ag(I) in CH_3CN (total ligand concentration: 10^{-4} M). Stoichiometric ratio: (a) Fe:Ag:L^1 = 1:1:2, (b) Fe:Ag:L^1 = 1:2:2, and (c) Fe:Ag:L^1 = 2:2:2 (*: cluster peaks).

by the two tridentate units of L^1 (structures **IV** and **V**). However, significant variations of the intensity of the $\pi_1 \rightarrow \pi^*$ transitions together with the red-shift of the lowest energy $\pi_1 \rightarrow \pi^*$ are a good indication of the coordination of Ag(I) to the complex[15] which is confirmed by the detailed ^{1}H-NMR analysis of $[FeAg(L^1)_2]^{3+}$ in CD_3CN ($\approx 10^{-2}$ M, decomplexation $\approx 5\%$). The ^{1}H-NMR spectrum of $[FeAg(L^1)_2]^{3+}$ displays 26 signals in agreement with a C_2-symmetrical complex compatible with structures **IV** and **V** (Figure 1). Comparison with the spectrum of $[Fe(L^1)_2]^{2+}$ shows that the coordination of Ag(I) does not strongly modify the protons of the tridentate site except for H_9 as previously observed with $[Zn_2(L^1)_2]^{4+}$ (Table 3) but significantly alters the signals of the protons of the bidentate site. Detailed NOEDIF and NOESY experiments clearly establish that the conformations of the bidentate units change from transoïd to cisoïd upon complexation to Ag(I) (NOE effect between Me_2-H_3 in $[FeAg(L^1)_2]^{3+}$) and H_9 lies between H_5 and H_6 in the shielding region of the benzimidazole ring of the bidentate unit (upfield shift:0.14 ppm) as described for $[Zn_2(L^1)_2]^{4+}$ (Scheme 1). However, we do not observe the expected upfield shift[11,15] for Me_1 since the ionic radius of Ag(I) (115 pm) is significantly larger than that of Zn(II) (74 pm).[39] We can conclude that $[FeAg(L^1)_2]^{3+}$ adopts the C_2-symmetrical helical structure **IV** where Fe(II) is coordinated by the two tridentate units and Ag(I) occupies the pseudotetrahedral site formed by the two bidentate units. Molecular mechanics calculations using the X-ray crystal structures of $[Fe(L^3)_2](CF_3SO_3)_2$[27] and $[Cu(L^4)_2]ClO_4$[15] as building blocks and CHARMM V23.f2 program[35] show that the

(39) Shannon, R. D. *Acta Crystallogr.* **1976**, *A32*, 751–767.

Scheme 1

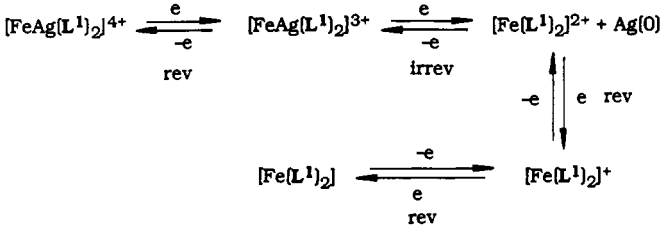

pseudo-C_2-symmetrical helical structure found for $[FeAg(L^1)_2]^{3+}$ lies in a minimum of energy and that the geometrical conformations of the diphenylmethane spacers are in good agreement with those depicted in Scheme 1 and observed by ^{1}H-NMR spectroscopy. However, the arrangement of the bidentate ligands around Ag(I) is severely distorted from ideal tetrahedral geometry as a result of constraints in the ligand backbone which may explain the low affinity of Ag(I) for $[Fe(L^1)_2]^{2+}$ (Figure 5).

Slow diffusion of ether into a concentrated acetonitrile solution allows the almost quantitative isolation of violet needles whose elemental analyses correspond to $[FeAg(L^1)_2](ClO_4)_3 \cdot 4H_2O$. The crystals are readily soluble in acetonitrile and give spectra (ES-MS, UV–vis, ^{1}H-NMR) identical to those obtained for $[FeAg(L^1)_2]^{3+}$ formed in situ. $[FeAg(L^1)_2](ClO_4)_3 \cdot 4H_2O$ is oxidized on a platinum disk electrode in a reversible monoelectronic wave at $E_{1/2}$ = 0.84 V vs SCE in CH_3CN + 0.1 M $TBAPF_6$ (Fe(III)/Fe(II); $E_p^a - E_p^c$ = 70 mV). This behavior parallels that of $[Fe(L^1)_2]^{2+}$ ($E_{1/2}$ = 0.83 V) and $[Fe(L^3)_2]^{2+}$ ($E_{1/2}$ = 0.76 V) in the same conditions. Upon complexation of Ag(I), no significant change is observed for the Fe(III)/Fe(II) reduction potential and for the two successive reduction waves centered on the coordinated tridentate units[26,40] which confirms that the coordination sphere around Fe(II) is very similar for $[Fe(L^1)_2]^{2+}$ and $[FeAg(L^1)_2]^{3+}$. The redox behavior of $[FeAg(L^1)_2](ClO_4)_3 \cdot 4H_2O$ is summarized in Scheme 1.

Heterotrinuclear Complexes with L^2. L^2 represents an extension of L^1 where two bidentate units, designed for tetrahedral coordination to Ag(I), are connected to the central tridentate unit. ES-MS titrations of L^2 with $AgClO_4 \cdot H_2O$ in acetonitrile for metal:ligand ratio between 0.1 and 2.0 give rather complicated spectra where we observe the successive formation of four homonuclear complexes $[Ag_n(L^2)_2]^{n+}$ (n = 1–4) as previously reported for substituted septipyridine (another septadentate ligand) which also forms a tetranuclear complex $[Cu_4(septipy)_2]^{4+}$ in acetonitrile.[13] ES-MS titrations of L^2 with $Fe(ClO_4)_2 \cdot 6H_2O$ shows the expected formation of $[Fe(L^2)_2]^{2+}$ (m/z = 838) as the only significant species for Fe(II):ligand ratio in the range 0.1–1.0. In large excess of Fe(II) (Fe(II)/$L^2 \geq 1.5$), we observe small peaks corresponding to $[Fe_2(L^2)_2]^{4+}$ (m/z = 433) (and its adduct ions with one and two ClO_4^-) but no trace of $[Fe_3(L^2)_2]^{6+}$. When L^2 is titrated by a stoichiometric 1:2 mixture of $Fe(ClO_4)_2 \cdot 6H_2O$ and $AgClO_4 \cdot H_2O$ (M_{tot}:L^2 between 0.2 and 3.0), we observe only three complexes: the mononuclear $[Fe(L^2)_2]^{2+}$ and the two heteronuclear complexes $[FeAg(L^2)_2]^{3+}$ (m/z = 595) and $[FeAg_2(L^2)_2]^{4+}$ (m/z = 473). Detailed spectrophotometric titrations of L^2 with $Fe(ClO_4)_2 \cdot 6H_2O$ or with $Fe(ClO_4)_2 \cdot 6H_2O$:$AgClO_4 \cdot H_2O$ mixtures and titrations of $[Fe(L^2)_2]^{2+}$ with $AgClO_4 \cdot H_2O$ in acetonitrile give spectrophotometric data which can be satisfactorily fitted with equilibria 4–7 (RMS deviation between calculated and observed absorbance; 0.003 or less):

$$Fe^{2+} + 2L^2 \leftrightarrow [Fe(L^2)_2]^{2+} \qquad \log(\beta_{12}) = 10.9(3) \quad (4)$$

$$2Fe^{2+} + 2L^2 \leftrightarrow [Fe_2(L^2)_2]^{4+} \qquad \log(\beta_{22}) = 14.6(3) \quad (5)$$

(40) Braterman, P. S.; Song, J. I.; Peacock, R. D. *Inorg. Chem.* **1992**, *31*, 555–559.

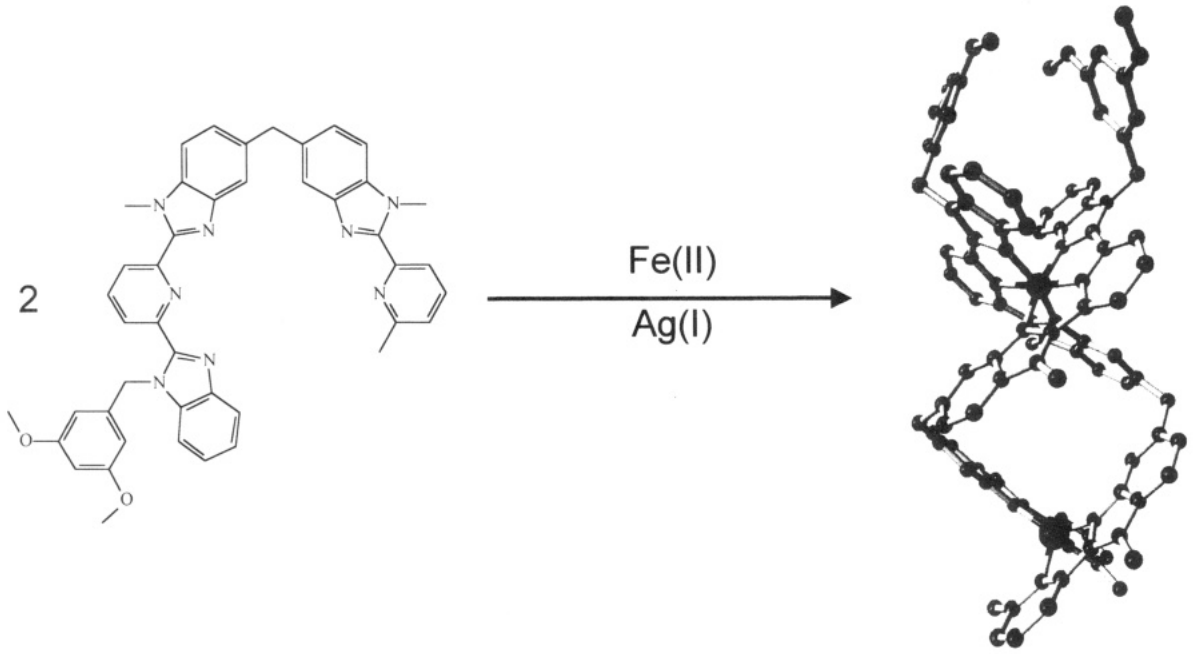

Figure 5. Self-assembly of double-helical heterodinuclear $[FeAg(L^1)_2]^{3+}$. The depicted structure of the complex corresponds to that found by molecular mechanics minimization using CHARMM V23.f2 program.[35]

$$[Fe(L^2)_2]^{2+} + Ag^+ \leftrightarrow [FeAg(L^2)_2]^{3+} \qquad \log(\beta) = 5.5(4) \tag{6}$$

$$[Fe(L^2)_2]^{2+} + 2Ag^+ \leftrightarrow [FeAg_2(L^2)_2]^{4+} \qquad \log(\beta) = 9.9(4) \tag{7}$$

$[Fe(L^2)_2]^{2+}$ is significantly less stable than the analogous complex with L^1 probably as a result of steric hindrance of the two bulky bidentate groups symmetrically bound to the 5-position of the benzimidazole rings of the tridentate units, but Ag(I) shows greater affinity for $[Fe(L^2)_2]^{2+}$ compared to $[Fe(L^1)_2]^{2+}$ as expected from statistical considerations[41] and in qualitative agreement with the ES-MS results.

The electronic spectrum of $[Fe(L^2)_2]^{2+}$ is very similar to that of $[Fe(L^1)_2]^{2+}$ and displays the typical features associated with pseudo-octahedral coordination of the two tridentate units to Fe(II).[26,27,31] However, the absence of 3,5-dimethoxybenzyl groups in L^2 removes the high energy shoulder observed in the $\pi_1 \rightarrow \pi^*$ band of $[Fe(L^1)_2]^{2+}$ (Table 2).[26] The ^{1}H-NMR spectrum of $[Fe(L^2)_2]^{2+}$ displays the 15 signals expected for a D_{2d}-symmetrical complex of structure **VIII**: the methylene protons H_7,H_8 are enantiotopic[14] and H_{13} is shifted downfield ($\Delta\delta$ = 0.41 ppm)[26,33] and H_9 upfield ($\Delta\delta$ = 2.18 ppm)[26,34] compared to L^2. NOEDIF and NOESY studies confirm that Fe(II) is bound to the tridentate units which adopt a cis–cis conformation (cross peaks between Me_3-H_{12}), while the bidentate units still maintain the transoïd arrangement of the coordinating nitrogen atoms. Upon complexation to Ag(I) to give $[FeAg_2(L^2)_2]^{4+}$, the electronic spectrum is not significantly modified except for a red-shift (230 cm^{-1}) of the MLCT Fe(II) $\rightarrow \pi^*$ which indicates that Fe(II) still occupies the octahedral site, but coordination of Ag(I) slightly modifies the electronic properties of the final complex (Figure 7).

The ^{1}H-NMR spectrum of $[FeAg_2(L^2)_2]^{4+}$ in CD_3CN displays 15 signals with enantiotopic A_2 spin systems for the methylene probes as previously observed for $[Fe(L^2)_2]^{4+}$ which imply a similar D_{2d}-symmetrical complex inconsistent with the three possible D_2-symmetrical structures **IX**, **X**, and **XI**. Fast exchange between enantiomers on the ^{1}H-NMR time scale explains the NMR data, and cooling down the sample to 253 K slows down the exchange process and leads to the observation of diastereotopic signals for H_7 and H_8 in agreement with structures **IX**–**XI**.[14] Similar exchange between enantiomers at room temperature has been previously reported for dinuclear double-helical and side-by-side complexes with Cu(I).[14] NOE measurements with $[FeAg_2(L^2)_2]^{4+}$ shows the expected cisoïd conformations of both tridentate and bidentate units confirming the coordination of Ag(I) to the complex. NOEDIF and NOESY spectra are poorly resolved as a result of chemical exchange at room temperature,[42] but they show a significant interaction between H_9 and H_6 and only a weak interaction between H_9 and H_5. However, H_9 shows the typical upfield shift ($\Delta\delta$ = 0.19 ppm) associated with the helical torsion of the diphenylmethane spacer which strongly suggests that $[FeAg_2(L^2)_2]^{4+}$ adopts the structures **IX** or **XI**. Unfortunately, our ^{1}H-NMR results cannot distinguish between the helical **IX** and the catenate **XI** structures which belongs to the same point group although they display different topologies.

Slow diffusion of methanol into a concentrated solution of $[FeAg_2(L^2)_2]^{4+}$ in acetonitrile gives violet pellets whose elemental analysis corresponds to $[FeAg_2(L^2)_2](ClO_4)_4{\cdot}4H_2O$. The crystals are readily soluble in acetonitrile and give spectra (ES-MS, UV–vis, ^{1}H-NMR) identical to those obtained for $[FeAg_2(L^2)_2]^{4+}$ formed in situ. $[FeAg_2(L^2)_2](ClO_4)_4{\cdot}4H_2O$ undergoes very similar redox processes at the platinum disk electrode to those described for $[FeAg(L^1)_2](ClO_4)_3{\cdot}4H_2O$ (Scheme 1). However, the Fe(III)/Fe(II) potential in $[FeAg_2(L^2)_2](ClO_4)_4{\cdot}4H_2O$ is less positive by 100 mV which reflects a destabilization of Fe(II) for this complex. Two successive quasi-reversible monoelectronic reduction waves centered on the coordinated tridentate units[26,40] are observed at negative potentials ($E_{1/2}$ = –1.11 and –1.57 V) as previously described for $[FeAg(L^1)_2](ClO_4)_3{\cdot}4H_2O$, but shifted by 40 and 100 mV, respectively, toward negative values. These observations, together with the red-shift of the MLCT transition and the stabilization of Fe(II) suggest that the LUMO for $[FeAg_2(L^2)_2](ClO_4)_4{\cdot}4H_2O$ lies at lower energy.[26,43]

Discussion

Previous work with homoleptic ligands showed that the diphenylmethane spacer was ideally suited for the development

(41) Sharma, V. S.; Schubert, J. *J. Chem. Educ.* **1969**, *46*, 506–507. Sigel, H. *Angew. Chem., Int. Ed. Engl.* **1975**, *14*, 394–402.
(42) Sanders, J. K. M.; Hunter, B. K. *Modern NMR Spectroscopy* 2nd ed.; Oxford University Press: Oxford, New York, Toronto, 1993; p 197.
(43) Figard, J. E.; Petersen, J. D. *Inorg. Chem.* **1978**, *17*, 1059–1063. Malouf, C.; Ford, P. C. *J. Am. Chem. Soc.* **1977**, *99*, 7213–7221.

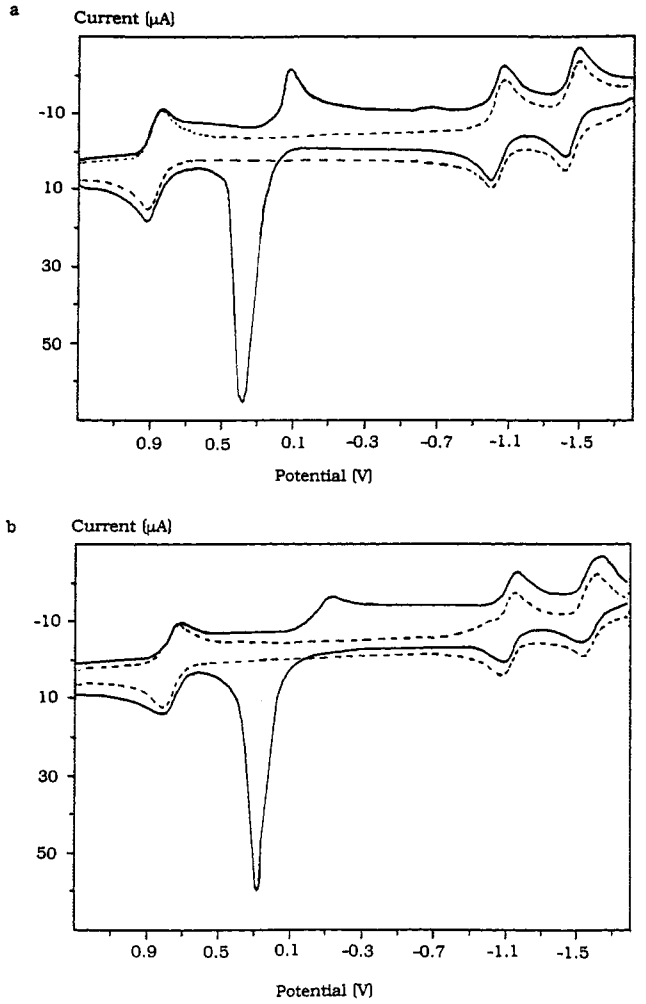

Figure 6. Cyclic voltammograms of (a) $[Fe(L^1)_2]^{2+}$ (dotted line) and $[FeAg(L^1)_2]^{3+}$ (full line) and (b) $[Fe(L^2)_2]^{2+}$ (dotted line) and $[FeAg_2(L^2)_2]^{4+}$ (full line) in CH_3CN + 0.1 M $TBAPF_6$. Potentials are given vs SCE.

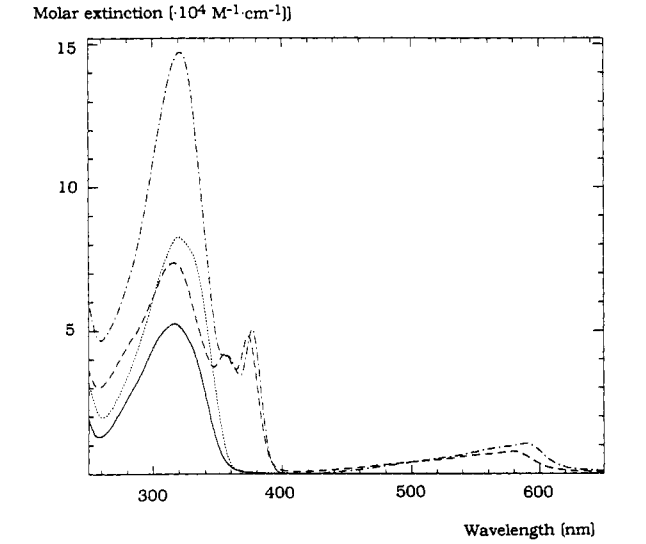

Figure 7. Electronic spectra of L^1 (full line), L^2 (dotted line), $[FeAg(L^1)_2]^{3+}$ (dashed line), and $[FeAg_2(L^2)_2]^{4+}$ (alternated line) in CH_3CN at 20 °C.

of segmental ligands designed for the self-assembly of helical homonuclear complexes.[15,19] The use of different coordinating units connected to the spacer in L^1 and L^2 significantly improves the coordination possibilities[20] but still maintains the constraints induced by the diphenylmethane spacer: (i) flexibility limited to two benzimidazole-CH_2 torsional angles and (ii) helical twist between the binding units. Accordingly, the formation of mononuclear $[ML]^{n+}$ complexes is unfavorable and indeed was never observed during ES-MS titrations of L^1 and L^2 with various metal ions, but the formation of complexes containing two ligands ($[M(L^i)_2]^{n+}$, $[M_2(L^i)_2]^{2n+}$, etc.; i = 1, 2) or three ligands ($[M(L^i)_3]^{n+}$, $[M_2(L^i)_3]^{2n+}$, etc.; i = 1, 2) may be considered together with many structural possibilities for each complex (Figure 1). Fortunately, a judicious matching of the ligand binding possibilities and the stereochemical preferences of the metal ions limits the possible structures. For L^1 and L^2, the tridentate unit favors the formation of pseudo-octahedral complexes[26,27] and the use of Fe(II) leads, under stoichiometric conditions, to the selective formation of the stable C_2-symmetrical head-to-head $[Fe(L^1)_2]^{2+}$ and the D_{2d}-symmetrical $[Fe(L^2)_2]^{2+}$ complex where Fe(II) is coordinated by the two tridentate units belonging to the different strands. Formation of rather unstable $[Fe_2(L^i)_2]^{4+}$ (i = 1, 2) in excess of metal indicates that the remaining bidentate units have only low affinities for Fe(II). Similarly, Co(II) and Zn(II) react with L^1 to give stable C_2-symmetrical head-to-head $[M(L^1)_2]^{2+}$ complexes (M = Co, Zn) where M is pseudo-octahedrally coordinated by the two tridentate units. However, Co(II) and Zn(II) have greater affinities for tetrahedral coordination[29] and form stable dinuclear head-to-head double-helical C_2-complexes $[M_2(L^1)_2]^{4+}$ (M = Co, Zn) where one metal ion is pseudo-octahedrally coordinated by the two tridentate units and the other metal ion occupies the remaining pseudotetrahedral site defined by the bidentate units of the strands (structure **IV**, Figure 1). There were no signs of mixtures of isomers (head-to-tail **VI**, **VII** or side-by-side **V**, Figure 1) nor of complexes with different stoichiometries during the self-assembly process, except for traces of $[M(L^1)_3]^{2+}$ (M = Co, Zn) in large excess of ligand.

The bidentate units of L^1 and L^2 favor the formation of pseudotetrahedral complexes,[11,15] and we could expect the formation of $[M(L^i)_2]^{+}$ with Ag(I) or Cu(I) (i = 1, 2). Such a complex is only observed as a minor species for L^2, and the dinuclear $[Ag_2(L^i)_2]^{2+}$ (i = 1, 2) represents the major complex in solution with both ligands.

These observations show that both octahedral metal ions (Fe(II), Co(II), Zn(II)) and tetrahedral metal ions (Ag(I), Cu(I)) have specific preferences for the tridentate binding unit in L^1 and L^2 which limits the application of this self-assembly process for the synthesis of heteronuclear complexes. However, Fe(II) displays a significantly greater affinity for the tridentate unit compared to Ag(I), and the use of stoichiometric equimolar mixtures of Fe(II)/Ag(I) leads to the selective formation of the double-helical heteronuclear complex $[FeAg(L^1)_2]^{3+}$ (Figure 5). For L^2, we observe the selective formation of the D_2-symmetrical heteronuclear complex $[FeAg_2(L^2)_2]^{4+}$ where Fe(II) lies in the pseudo-octahedral site and Ag(I) in the remaining pseudotetrahedral sites compatible with both double-helical (**IX**) and catenate (**XI**) structures. The thermodynamic data show that the selectivity of the self-assembly process strongly depends on the stoichiometric conditions, and we may expect the substitution of Fe(II) by excess of Ag(I) according to equilibria 8 and 9:

$$[FeAg(L^1)_2]^{3+} + Ag^+ \leftrightarrow [Ag_2(L^1)_2]^{2+} + Fe^{2+} \qquad \log K \approx -3.5 \quad (8)$$

$$[FeAg_2(L^2)_2]^{4+} + 2Ag^+ \leftrightarrow [Ag_4(L^2)_2]^{4+} + Fe^{2+} \quad (9)$$

This is indeed observed by ES-MS, and peaks corresponding to $[Ag_2(L^1)_2]^{2+}$ and $[Ag_4(L^2)_2]^{4+}$ appear in the spectra when excess Ag(I) is added to $[FeAg(L^1)_2]^{3+}$ (Figure 4b) and $[FeAg_2(L^2)_2]^{4+}$ in acetonitrile.

For concentrations compatible with NMR measurements (5×10^{-3}–2×10^{-2} M), we found that decomplexation is only ≈5%,

and the spectra reflect the structure of the heteronuclear complexes in solution. The systematic use of symmetry arguments, diastereotopic probes, and detailed analysis of the chemical shifts allows the unambigous characterization of the coordination sphere around the metal ions. We have found that NOE effects associated with the transoïd → cisoïd interconversions which occur upon complexation of oligo-multidentate ligands to metal ions[11-15,32] are particularly useful for the study of the coordination of the different units to the metal ions, and this technique allows the easy characterization of mononuclear complexes $[M(L^1)_2]^{2+}$ (M = Fe, Zn) and $[Fe(L^2)_2]^{2+}$ where only one binding unit is coordinated to the metal ion.

Comparison of our heteronuclear self-assembly processes with the formation of the heteronuclear complex $[CoAg(quinquepy)_2]^{3+}$ previously described by Constable and co-workers[18] is very difficult since no thermodynamic data were reported and $[CoAg(quinquepy)_2]^{3+}$ was obtained by stoichiometric mixing of $[Co(quinquepy)(MeOH)_2]^{2+}$ and $[Ag(quinquepy)]^+$ at high concentrations which corresponds to the conditions in which we observe only the selective self-assembled heteronuclear complex $[FeAg(L^1)_2]^{3+}$ in solution. As reported for $[CoAg(quinquepy)_2]^{3+}$, ^{1}H-NMR data and electronic spectra show that L^1 and L^2 always adopt head-to-head arrangements in the heteronuclear complexes and in the homodinuclear $[Zn_2(L^1)_2]^{4+}$ although a head-to-tail structure was reported for the distorted analogous complex $[Pd_2(quinquepy)_2]^{4+}$.[44] The major difficulty associated with the structural characterization of our complexes lies in the discrimination between side-by-side, helical, and catenate complexes which belong to the same point group (structures **IV**, **V**, **IX**, **X**, and **XI**). This problem was not encountered by Constable and co-workers[18] since the lack of a spacer between the pyridine rings in quinquepy prevents side-by-side coordination, and no catenate is possible for this pentadentate ligand with octahedral metal ions. Molecular models and molecular mechanics calculations show that the diphenylmethane spacer adopts different geometrical conformations in helical and side-by-side complexes which are associated with different NOE signals and "through space" shielding of H_9. Detailed analysis of the ^{1}H-NMR spectra and NOE effects imply that $[FeAg(L^1)_2]^{3+}$ and $[Zn_2(L^1)_2]^{4+}$ adopt the double-helical structure as found in $[CoAg(quinquepy)_2]^{3+}$.[18] These complexes may be obtained analytically pure as their perchlorate salts by crystallization from acetonitrile. Repeated attempts to obtain X-ray quality crystals of the complexes with L^1 have been unsuccessful probably as a result of the presence of lipophilic 3,5-dimethoxybenzyl groups which increase the solubility[14] and allow the studies in solution but hinder the formation of well-ordered crystals.[9] For $[FeAg_2(L^2)_2]^{4+}$, double-helical and catenate arrangements display similar conformations of the diphenylmethane spacer, and discrimination between these structures is very difficult in solution. The dark violet pellets of $[FeAg_2(L^2)_2](ClO_4)_4$ are not suitable for X-ray structural determination, but the replacement of ClO_4^- by PF_6^- gives larger prisms which are currently under investigation and could allow the discrimination between structures **IX** and **XI** in the solid state.

Conclusions

L^1 and L^2 combine two well-defined different binding units with a spacer which allows the ligands to act as bidentate–tridentate ligands ideally suited for the formation of heterodi- and heterotrinuclear complexes.[15] Strict self-assembly, as defined by Lindsey,[46] of heteronuclear complexes $[FeAg(L^1)_2]^{3+}$ and $[FeAg_2(L^2)_2]^{4+}$ is observed in acetonitrile, but detailed speciation and thermodynamic studies of the processes show that the selective formation of the complexes depends on stoichiometric conditions (the ratio of Fe(II):Ag(I) and total concentration). This situation arises from the considerable affinities of both Fe(II) and Ag(I) for the tridentate coordinating unit even though Fe(II) forms more stable complexes. Fortunately, the reverse situation is observed for the bidentate coordinating units which eventually leads to the formation of the desired pure heteronuclear complexes under suitable conditions.

At first sight the relatively low selectivity of the two different sites may be disappointing. It should be noted however that the two sites differ only in their denticity, the ligating atoms (imine nitrogens) and the chelate bite angle remaining constant. Greater selectivity for different metals may be introduced by modification of the ligating atoms (to distinguish class A and class B metals) and by modification of the chelate bite angle, allowing selection based on metal size and stereochemical preference.

Strict self-assembly of helical heteronuclear complexes requires the usual conditions for homonuclear complexes[11-15] together with the three following points: (i) thermodynamic equilibrium between the various species of the self-assembly process, (ii) different affinities of the various metal ions for the different coordinating units, and (iii) sufficient discrimination in the affinity of each metal ions for the same binding unit. Following these criteria it should be possible to introduce selectively various metal ions in self-assembled helical architectures under thermodynamic control. This offers new possibilities for the development of molecular light-conversion devices based on heteronuclear helical lanthanide complexes.[9]

Acknowledgment. We gratefully acknowledge Dr. Elisabeth Rivara for recording the NOEDIF and 2D-NOESY spectra. This work is supported through grants from the Swiss National Science Foundation.

(44) Constable, E. C.; Elder, S. M.; Healy, J.; Ward, M. D.; Tocher, D. A. *J. Am. Chem. Soc.* **1990**, *112*, 4590–4592.

(45) Bilyk, A.; Harding, M. M. *J. Chem. Soc., Dalton Trans* **1994**, 77–82.

(46) Lindsey, J. S. *New J. Chem.* **1991**, *15*, 153–180.